RF Localization of RFIDs Using a Robotic Arm

Isaac Perper, Tara Boroushaki
Massachusetts Institute of Technology
{iperper,tarab}@mit.edu

ABSTRACT

We present the design, implementation, and evaluation of a robotic system that can localize items through occlusions and grasp them. Our system identifies and locates RFID tagged objects in non-line-of-sight scenarios.

The system relies on an eye-in-hand camera, a wrist mounted antenna, and batteryless RFID tags attached to objects of interest. It has two main components: (1) an RFID localization system that is mounted on the robot and uses the arm movement to gather data from different positions to localize the RFID tagged item and (2) an RF-visual deep neural network that can find and execute a grasping strategy.

We implemented and evaluated an end-to-end physical prototype using a UR5e robotic arm, RealSense depth camera, BladeRF xA4, a log-periodic antenna and a patch antenna. We demonstrate it can localize RFID tagged items and grasp the identified item.

1 INTRODUCTION

Accurate and precise localization of objects is essential for tasks such as manufacturing, robotic manipulation, and inventory management[16]. For example, with precise location estimates a robot on an assembly line can grab the correct parts out of a box and fasten them correctly to the manufactured product. Moreover, after completing the task, the robot can check the location of that same object again to confirm it was applied in the correct location.

Many modern approaches to localization have focused on cameras to segment and track objects of interest in images, often with RGB-D data [11]. Despite all these advances, however, visual-based estimations of location are limited by the fact that the objects of interest must be in line-of-sight of the camera. Occluded objects in boxes or under other items are impossible to find directly.

RFID localization addresses these limitations by estimating the position of RFID tags with RF signals. RFIDs are low-cost, batteryless stickers that have already been deployed on billions of items around the world. RF signals traverse through many common materials, meaning location estimates can be determined without a line-of-sight. Additionally, recent work in this domain has demonstrated sub-centimeter localization precision - making it directly useful for many of the tasks described above [15, 16]. Traditionally, RFID localization has required taking RF measurements from multiple antennas at predetermined, fixed points in space, such that multiple distance estimates can trilaterate the location of the RFID.

However, there's nothing inherent to the design of these system about fixing multiple antennas at specific locations. In fact, the more measurements you can take, the more robust the system is to noise, so leveraging antenna motion for spatial diversity of measurements can be a promising approach. More importantly, the system can be smarter. Measurements could be taken a certain locations to maximize the 'information gain' of each successive measurement. In real-time, the localization system could be adapting measurement positions, orientations, and signal gain to get the most useful and accurate distance measurements.

One can imagine the applications and benefits of such an approach to robotic manipulation tasks. Firstly, a robotic arm can already move to a wide range of poses, and capture the location of those poses accurately. With an antenna attached to a robotic arm, the robot can leverage its movement to take multiple measurements as needed. This procedure could even be encoded into the trajectory optimization itself. Secondly, a robot with RFID localization is able to complete many previously difficult or inefficient tasks. Objects can be identified and grasped despite being occluded from camera view [13], or the robot can perform mechanical search, efficiently finding all objects of a certain class in the environment.

Additionally, mobile systems can benefit from a motion-based RFID localization approach. Mobile robots could determine the relative location of an RFID, and simply navigate in space to capture more measurements as needed.

In this paper we aim to explore these applications by fixing an antenna to a robotic arm, localizing an RFID by moving the antenna in space, and using the acquired location to grasp the object the RFID is attached to. We also discuss how the fundamental RFID location-from-motion approach can be improved and seamlessly integrated as a standard robotics tool.

2 RELATED WORK

RFID is a relatively mature technology that has seen widespread adoption by many industries as barcode replacement over the past few years in retail, manufacturing, and warehousing [3]. Today's UHF (Ultra-High Frequency) RFIDs cost as little as 3-cents and don't require any batteries. A wireless device called a reader can read and uniquely identify RFIDs from up to 9 m and through occlusions.

Recognizing the potential for RFIDs in robotics, researchers have developed systems that leverage RFIDs as location markers to facilitate navigation [9, 12, 18] and to guide a mobile robot toward grasping [4–7, 21, 21].

Furthermore, leveraging motion to gather RF location estimates has been shown in a variety of work, generally in a SAR-based approach [2, 10, 19, 23, 25]. RF-SML [10] moves an antenna along a linear-slide to localize RFID tags based on angle-of-arrival, achieving centimeter level precision. However, much like most SAR approaches, restricting movement to a precise linear track is essential to get good estimates. [2] builds a novel system of two robot-mounted RFID readers, and measures robot vehicle movements to inform a SAR-based 3D localization at tens of centimeter precision. [14, 23, 24, 26] are other applications of mobile robots localizing RFID tags. In this paper we explore a robotic arm mounted antenna to enable grasping in particular.

3 DESIGN

3.1 Background on RFID Distance Estimation

Before explaining how the overall system works, it's important to understand the fundamentals of RFID localization. RFIDs are small, battery-less tags consisting of an antenna, power-harvesting circuit, and control chip. A RFID reader can transmit a query signal, to which the RFID can respond to. To respond, the RFID tag backscatters the query signal, either absorbing the signal energy so it is not reflected, or reflecting it back to the environment. For estimating the distance of the RFID tag, there are many approaches but this paper utilizes the frequency-hopping approach found in [16]. The approach can be summarized as follows.

First the RFID is queried at multiple frequencies, and channel estimates are extracted from the response. The difference between these reflective and non-reflective channels is the channel to the RFID tag and back. The multiple frequencies are chosen the make this a wideband channel estimate. With enough bandwidth and some additional processing, the time-of-flight (ToF) of the direct path signal from transmitter->tag->receiver can be estimated. Finally, distance is easily recovered using the relationship:

$$d_{est} = \frac{\Delta t_{\text{ToF}}}{2\pi}$$

[16] can be referenced for details on how the distance estimates are calculated and enhanced with super resolution.

3.2 Position Estimates

The high-level procedure to acquire an accurate location from multiple measurements is shown in Fig. 1.

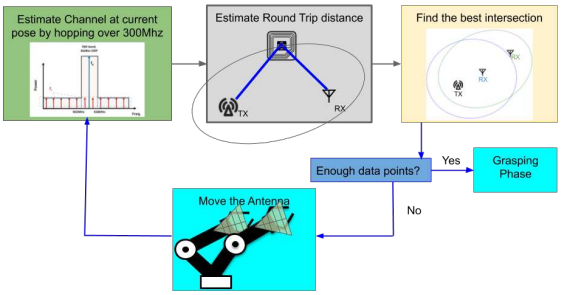

Figure 1—The Localization Procedure. First, the system gathers channel and distance estimates at a few locations. Based on the estimated location, it decides whether to gather more measurements by taking more spatially diverse distance estimate. If it has enough points, it uses the location estimate to perform grasping.

The robot starts by collecting three distance measurements, such that the position optimization can output an estimate of the 3D location of the tag. However, the roundtrip distance measurements often have error from environment noise, multipath, and other factors. Thus, we can measure the residuals from the position estimate, and determine if additional measurements are needed to improve the accuracy.

3.3 Grasping

Once an accurate position estimate of the RFID-tagged object is determined, grasping can occur. The robot moves directly above the estimated position, looking downward with the camera. This phase of system uses a model free deep-reinforcement learning network that aims to identify optimal grasping affordances from RGB-D, using the RFID's location as an attention mechanism. Because the camera image is used in this stage to find the best grasping strategy, the position estimate from Section 3.2 can have small errors without affecting the grasping performance.

The input to the Deep Neural Network are RF-Kernel, depth and RGB Heightmaps. Heightmaps are computed by extracting 3D point cloud from RGB-D images and projecting the images orthographically, parallel to the table top. The RGB and depth heightmap represent color and height from tabletop respectively. The RFID location is also used to construct an RF kernel, a 2D Gaussian centered around tagged item estimated location, whose standard deviation represents RF localization errors. The system incorporates RF-based attention through two main strategies:

- *RF-based Binary Mask.* The RGB and depth heightmaps are cropped to a square around the RFID's location (11cm×11cm). This pre-processing attention mechanism allows the network to focus on the vicinity of the target object and compute the affordance map with higher resolution and/or less computational complexity.
- *RF Kernel.* The kernel is fed to the network, and is also multiplied by DQN's last layer to compute the final affordance map. This increases the probability of grasping the target item.

The output of grasping network contains 16 maps for grasp, from which the system chooses the position and gripper rotation with highest probability of success.

4 IMPLEMENTATION

We implemented the system using two bladeRF xA4 software-defined radios (SDRs) [17], a UR5e robot arm, 2F-85 Robotiq gripper, and an Intel Real-Sense D415 depth camera mounted on the gripper. Fig. 2 shows these components and how they are connected on the robot. Currently the RFID transmitter antenna is placed at the base of the arm, and the receive antenna is placed at the robot wrist. The Realsense depth camera is also mounted on the wrist of the robot. However, with the small form factor of the bladeRF, the system could be entirely placed on the arm in the future.

The robot is controlled using Universal Robots ROS Driver on ROS kinetic. We used Moveit! [8] and OMPL [22] for planning scene and inverse kinematic solver. The code is implemented in both C++ and Python. Objects of interest are tagged with off-the-shelf UHF RFIDs (e.g., Alien tag [1])

4.1 bladeRF

The bladeRF platform was chosen as it's a more compact and cheaper than other SDRs, such as Ettus URSPs [20]. Multi-antenna RFID localization had already been achieved on USRPs, so the groundwork was in place to utilize the bladeRFs for RFID localization. However, there were numerous issues to overcome to improve the accuracy before the rest of the system could be implemented. The following subsections describe the important parts of the bladeRF implementation.

4.1.1 Hardware. Besides the high-level hardware shown in Fig. 2, there were additional requirements. The bladeRF that sends the query to the RFID has a BT-100 power-amp on the transmitter, which allows it to power up that tag at sufficient distance. Additionally, that bladeRF also serves as the master clock, which it outputs to the second bladeRF. This is done to ensure the two devices are closely hardware synchronized. The two devices can actually be made more accurately synchronized with a trigger mechanism. However, this triggering wasn't in the scope of this paper. The transmit radio gains were set to their maximum, and the receive gains were adjusted to prevent clipping in the signal.

4.1.2 Frequency Hopping. To gather a wideband channel estimate, the second bladeRF takes narrowband channel estimates every 20MHz, starting at 800MHz and stopping at 1100 MHz. 300MHz gives enough accuracy in the time domain to achieve good ToF measurements. With the bladeRF, the high-level API is limited to 16 stored tuning frequencies, so measuring an even higher bandwidth was not explored for this paper, since we wanted to limit increasing the frequency spacing too much.

4.1.3 TX/RX Phase Synchronization. While implementing the frequency hopping, it was noted that the phase of the system did not behave as it should. Accurate phase estimates are necessary for accurate distance measurements, as shown by the relationship:

$$d_{\text{est}} = \lambda \frac{\theta}{2\pi}$$

However, the RX and TX of a single bladeRF device operate on different phase-locked loops (PLLs). Fig. 3 the simplified radio front-end of the bladeRF oscillator paths. PLLs operate by locking at a constant phase-offset from some reference signal. However, this constant offset is random, and thus the RX and TX signals would have an unknown phase offset between them, rendering the distance measurements inaccurate.

To illustrate the issue, imagine the phase of the TX and RX signals can be written as:

$$\theta_{TX} = \theta_{\text{initial}} + Y \qquad \theta_{RX} = \theta_{\text{final}} + X$$

where X and Y are random variables of $[0, 2\pi]$ offset, θ_{initial} is the unwrapped phase sent, and θ_{RX} is the unwrapped phase received.

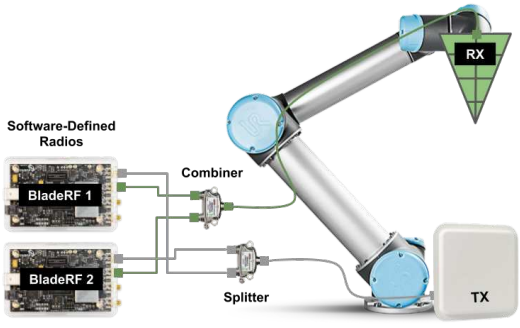

Figure 2—High Level Implementation. Two software radios connect to a wrist mounted antenna, and the arm moves around with the receiver antenna attached. The transmitter is placed at the base of the robot and is fixed in place.

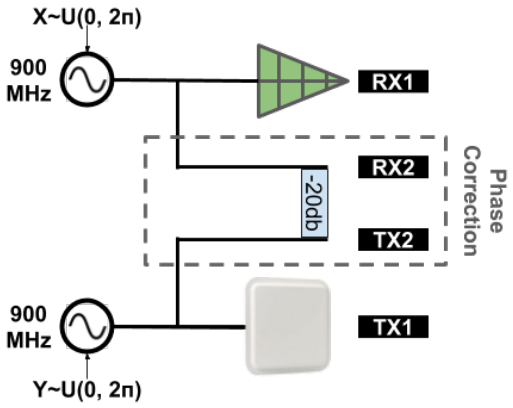

Figure 3—Correcting for random phase offset between TX and RX. The TX and RX frontends are on different PLLs, such that it is impossible to determine the change in phase of the sent and received signal. To resolve this, we loop the second TX output directly into the second RX input via an attenuator. This gives us a measurement of the phase offset to correct the over-the-air signal with.

Measuring the phase of the over-the-air signal can conventionally be done by subtracting the final phase from the initial phase of the system:

$$\theta_{RX} - \theta_{TX} = \Delta\theta + X - Y$$

Clearly the $X - Y$ offset must be corrected for. Luckily, the bladeRFs are MIMO capable devices with two TX and two RX ports. Fig. 3 shows the phase offset solution, where the extra pair of TX and RX ports are looped back on each other using an attennuator, with no other modifications. Now we have:

$$\begin{aligned}
\theta_{RX1} - \theta_{TX1} &= \Delta\theta + X - Y \\
\theta_{RX2} - \theta_{TX2} &= X - Y \\
\theta_{RX} - \theta_{TX} &= \theta_{RX1} - \theta_{TX1} - (\theta_{RX2} - \theta_{TX2}) \\
&= \Delta\theta
\end{aligned}$$

Now the recovered $\Delta\theta$ has been corrected, and can be used for accurate location estimates.

4.2 Antenna Design

The original RFID localization platform used RFID patch antennas for power-up and localization. That being said, a 850-6500 MHz log-periodic antenna was placed on the robot wrist, and it was small enough that the gripper was not obstructed. However, during testing the 850-6500MHz antenna did not give reliable or accurate distance measurements. While the exact cause was not determined, the larger log-periodic antenna built for 400-1000MHz achieved much stronger results. One theory is that the antenna gain improved the SNR of the RFID response. The current 400-1000MHz antenna sits much closer to the end of the gripper, making grasping more difficult, although still achievable. For mounting the antenna, a hole was drilled between the traces on the antenna through the PCB. This was mounted on the robot wrist with an action camera mount, and the 3D wrist-antenna transformation was measured. An omni-direction patch antenna was used for transmitting the query signal and frequency hops. This was placed near the base of the robot.

5 EVALUATION

The robot workspace is atop a table with dimensions of 0.8m×1.2m. We consider two metrics: *1) Round Trip Distance Accuracy:* the accuracy of the system in measuring the round trip distance which is the distance from transmitter antenna to RFID tag plus the distance from RFID tag to the receiver antenna. *2) 2D Localization Accuracy:* The accuracy of localizing the RFID tag position in X and Y axis.

5.1 Quantitative Results

We evaluated the system by placing the RFID tagged item in various locations and moving the robot arm with its wrist mounted antenna and camera on different trajectories. We also varied the initial position of the robot across experimental trials.

a) Round Trip Distance Accuracy: We recorded the antenna's location when the channel estimate measurements was performed. By knowing the true location of RFID tagged item, the ground truth round trip distance from transmitted antenna to RFID tag and back to each antenna recorded position can be computed. We tested the system by putting the RFID tagged item in 3 different positions and localizing it. We placed the robot in an initial pose where the wrist-mounted antenna is aimed toward the approximate location of RFID tag. The robot arm moved in a straight path making frequent stops to get a channel estimate from different position. The total number of trials was 17. The median error of round trip distance was 0.0253 meter, and the mean error was 0.0029 meter.

2) 2D Localization Accuracy: Next, we evaluated the 2D localization accuracy of the system across the same experiments described above. Table 1 shows the results. The mean and median error of the localization shows that while the round trip distance accuracy is around 2.5 cm the system was able to estimate the location of tag with median error of 1 cm when provided enough data points. As the number of measurement points increases the system localization's accuracy improves.

	2 points	3 points	4 points
X-axis Mean Error	0.0162	0.0146	0.019
X-axis Median Error	0.0190	0.0115	0.01
Y-axis Mean Error	0.0207	0.0122	0.0106
Y-axis Median Error	0.02	0.0105	0.002

Table 1—Localization Error. The mean and median error of localization is each X and Y axis are reported above.

Fig. 4 shows how having multiple round trip distance estimate can help localizing the tagged item with accuracy higher than round trip distance estimation themselves.

5.2 Qualitative Results

Next, we show that our portable localization system can enable grasping the localized item. We recommend you see the video in Section 5.3 for demonstration. We placed a RFID tagged item on the table 16cm below robot's base. The robot moves in a predefined straight line and gathers measurements. The RFID localization system localizes the tagged item and and moves directly above the item. The attention mechanism biases the grasping network to perform a grasp on the localized object. We tested the system 2 times in this scenario and it was able to grasp the item of interest in the first attempt.

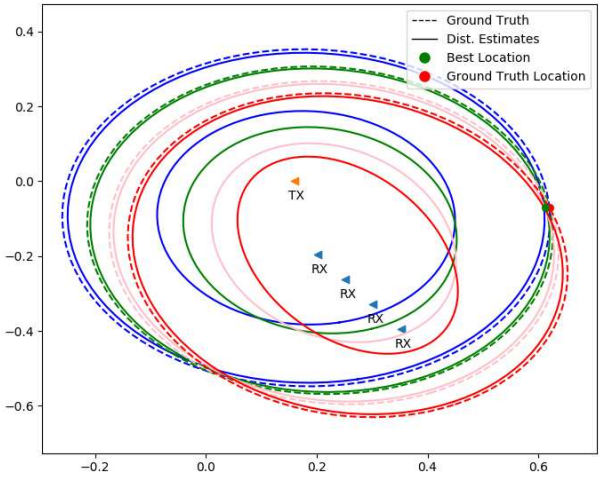

Figure 4—The distance inputs to the optimization visualized with ground truth. Every round trip distance estimate, from a RX antenna position, is visualized using undotted ellipse with a different color. The dotted ellipses are ground truth round trip distances. The wrist mounted antenna estimated the channel in 4 location shown by blue triangles. Each time, it determines two possible distance measurements: rounding up to nearest integer wavelength, and rounding down. The position optimization looks at all the pairings, and determines the most likely position as shown by green circle. The ground truth position of RFID is shown by red circle.

5.3 Video

A video of the robot localizing and grasping can be found here.

6 DISCUSSION & CONCLUSION

The paper shows that it is possible to use a robotic arm for RFID localization. Although there are accuracy and performance improvements to make in the future, the key ideas of gathering multiple distance estimates from a wrist-mounted antenna, calculating a location, and attempting grasping were well demonstrated. The most accurate x-y position estimates came from the experiments that took the most measurements (4), with median error of 0.01 m in the x-direction and 0.002 m in the y-direction. In fact, the mean and median errors strictly decrease with more measurements, suggesting that more can be done to characterize the limits of this trend. However, these results are nonetheless promising, as they indicate that the location errors are due to noise in the measurements that can be reduced with more points, rather than any fundamental issues with our experimental setup.

With a large number of measurement points, the experimental results suggest a potentially several-mm accurate system. However, acquiring all those points in an efficient and timely manner requires a faster frequency hopping system and other performance improvements.

Still, the roundtrip accuracy (1D measurements) was never replicated to a cm-level precision, even though this accuracy has been found with a similar codebase but on USRP N210 SDRs. Further exploring the reasons for this will be valuable for long-term usage of the bladeRF platform. Similarly, the bladeRFs are clearly more

limited in TX gain, and a long-term solution will be needed to increase the range.

Moving forward, there are numerous next steps that can build on this work. RF measurements using antenna movement for tasks such as localization and imaging has been well researched in a domain called synthetic aperture RADAR (SAR). One of the challenges with SAR is the need for highly accurate measurements of antenna location, and antenna movement is generally in a pre-defined linear or circular pattern. The diverse maneuverability of robotic arm could enable an adaptive SAR, where the antenna path is is determined via a RF-aware motion planning optimization. Similarly, quantifying the benefits of this system for grasping tasks, either in path efficiency or success rates can be a useful endeavor.

REFERENCES

[1] ALN-9640 Squiggle Inlay. www.alientechnology.com. Alien Technology Inc.

[2] F. Bernardini, A. Motroni, P. Nepa, A. Buffi, P. Tripicchio, and M. Unetti. Particle Swarm Optimization in Multi-Antenna SAR-based Localization for UHF-RFID Tags. In *2019 IEEE International Conference on RFID Technology and Applications (RFID-TA)*, pages 291–296, 2019. doi: 10.1109/RFID-TA.2019.8891990.

[3] Raghu Das. RFID Forecasts, Players and Opportunities 2019-2029. IDTechx, 2019.

[4] Travis Deyle, Cressel Anderson, Charles C Kemp, and Matthew S Reynolds. A foveated passive uhf rfid system for mobile manipulation. In *2008 IEEE/RSJ International Conference on Intelligent Robots and Systems*, pages 3711–3716. IEEE, 2008.

[5] Travis Deyle, Hai Nguyen, Matt Reynolds, and Charles C Kemp. Rf vision: Rfid receive signal strength indicator (rssi) images for sensor fusion and mobile manipulation. In *2009 IEEE/RSJ International Conference on Intelligent Robots and Systems*, pages 5553–5560. IEEE, 2009.

[6] Travis Deyle, Christopher J Tralie, Matthew S Reynolds, and Charles C Kemp. In-hand radio frequency identification (rfid) for robotic manipulation. In *2013 IEEE International Conference on Robotics and Automation*, pages 1234–1241. IEEE, 2013.

[7] Travis Deyle, Matthew S Reynolds, and Charles C Kemp. Finding and navigating to household objects with uhf rfid tags by optimizing rf signal strength. In *2014 IEEE/RSJ International Conference on Intelligent Robots and Systems*, pages 2579–2586. IEEE, 2014.

[8] Ettus Research, CDA-2990. https://moveit.ros.org/.

[9] Wail Gueaieb and Md Suruz Miah. An intelligent mobile robot navigation technique using rfid technology. *IEEE Transactions on Instrumentation and Measurement*, 57(9):1908–1917, 2008.

[10] Yue Jiang, Yongtao Ma, Hankai Liu, and Yunlei Zhang. RF-SML: A SAR-Based Multi-Granular and Real-Time Localization Method for RFID Tags. *Electronics*, 9 (9):1447, September 2020. ISSN 2079-9292. doi: 10.3390/electronics9091447. URL https://www.mdpi.com/2079-9292/9/9/1447.

[11] B. Kim, S. Xu, and S. Savarese. *Accurate Localization of 3D Objects from RGB-D Data using Segmentation Hypotheses*. 2013. Publication Title: Proceedings of the IEEE International Conference on Computer Vision and Pattern Recognition.

[12] Myungsik Kim and Nak Young Chong. Direction sensing rfid reader for mobile robot navigation. *IEEE Transactions on Automation Science and Engineering*, 6(1): 44–54, 2008.

[13] Junshan Leng. *RF-Guided Exploration for Robotic Manipulation*. PhD thesis, MIT, September 2020.

[14] Z. Liu, Z. Fu, T. Li, I. White, R. Penty, and M. Crisp. An ISAR-SAR based Localization Method using Passive UHF RFID System with Mobile Robotic Platform. In *2020 IEEE International Conference on RFID (RFID)*, pages 1–7, 2020. doi: 10.1109/RFID49298.2020.9244907.

[15] Zhihong Luo, Qiping Zhang, Yunfei Ma, Manish Singh, and Fadel Adib. 3D Backscatter Localization for Fine-Grained Robotics. In *16th USENIX Symposium on Networked Systems Design and Implementation (NSDI 19)*, pages 765–782, Boston, MA, February 2019. USENIX Association. ISBN 978-1-931971-49-2. URL https://www.usenix.org/conference/nsdi19/presentation/luo.

[16] Yunfei Ma, Nicholas Selby, and Fadel Adib. Minding the Billions: Ultra-wideband Localization for Deployed RFID Tags. In *Proceedings of the 23rd Annual International Conference on Mobile Computing and Networking*, pages 248–260, Snowbird Utah USA, October 2017. ACM. ISBN 978-1-4503-4916-1. doi: 10.1145/3117811.3117833. URL https://dl.acm.org/doi/10.1145/3117811.3117833.

[17] NUAND. bladeRF 2.0 Micro. URL https://www.nuand.com/bladerf-2-0-micro/.

[18] Sunhong Park and Shuji Hashimoto. Autonomous mobile robot navigation using passive rfid in indoor environment. *IEEE Transactions on industrial electronics*, 56 (7):2366–2373, 2009.

[19] L. Qiu, Z. Huang, N. Wirström, and T. Voigt. 3DinSAR: Object 3D localization for indoor RFID applications. In *2016 IEEE International Conference on RFID (RFID)*, pages 1–8, 2016. doi: 10.1109/RFID.2016.7488026.

[20] Ettus Research. USRP N210. URL https://kb.ettus.com/N200/N210.

[21] Longfei Shangguan and Kyle Jamieson. The design and implementation of a mobile rfid tag sorting robot. In *Proceedings of the 14th annual international conference on mobile systems, applications, and services*, pages 31–42, 2016.

[22] The Open Motion Planning Library. https://ompl.kavrakilab.org/.

[23] A. Tzitzis, S. Megalou, S. Siachalou, E. Tsardoulias, T. Yioultsis, and A. G. Dimitriou. 3D Localization of RFID Tags with a Single Antenna by a Moving Robot and "Phase ReLock". In *2019 IEEE International Conference on RFID Technology and Applications (RFID-TA)*, pages 273–278, 2019. doi: 10.1109/RFID-TA.2019.8892256.

[24] A. Tzitzis, S. Megalou, S. Siachalou, T. G. Emmanouil, A. Filotheou, T. V. Yioultsis, and A. G. Dimitriou. Trajectory Planning of a Moving Robot Empowers 3D Localization of RFID Tags With a Single Antenna. *IEEE Journal of Radio Frequency Identification*, 4(4):283–299, 2020. doi: 10.1109/JRFID.2020.3000332.

[25] Jue Wang and Dina Katabi. Dude, where's my card?: RFID positioning that works with multipath and non-line of sight. *ACM SIGCOMM Computer Communication Review*, 43(4):51–62, September 2013. ISSN 0146-4833. doi: 10.1145/2534169.2486029. URL https://dl.acm.org/doi/10.1145/2534169.2486029.

[26] R. Zhao, Y. Zhang, G. Wang, and D. Wang. Mobile Robot Localization using Rotating Synthetic Aperture RFID. In *2018 IEEE CSAA Guidance, Navigation and Control Conference (CGNCC)*, pages 1–6, 2018. doi: 10.1109/GNCC42960.2018.9019177.